Nanoscale

ROYAL SOCIETY OF CHEMISTRY

COMMUNICATION

View Article Online
View Journal | View Issue

Cite this: *Nanoscale*, 2020, **12**, 10987

Received 2nd April 2020,
Accepted 8th May 2020

DOI: 10.1039/d0nr02639e

rsc.li/nanoscale

A co-crystallization induced surface modification strategy with cyanuric acid modulates the bandgap emission of carbon dots†

Zhengjie Zhou, [a,b] Elena V. Ushakova, [c,d] Enshan Liu,[e] Xin Bao,[a,b] Di Li,[a] Ding Zhou,[a] Zhanao Tan, [e] Songnan Qu *[f] and Andrey L. Rogach [c,d]

Along the line of offering surface modification strategies to tune emission properties of carbon dots (CDs), a co-crystallization strategy with cyanuric acid (CA) was developed to modulate the bandgap emissions of CDs and produce highly emissive solid composite CD-based materials. The original blue emission of the CDs changed to a green emission of the CDs@CA crystals, which showed a high photoluminescence quantum yield of 62% and room temperature phosphorescence. The CA molecules firmly bonded to the surface of the CDs and cannot be disrupted by polar solvents or temperature stimuli under ambient conditions, which influenced electron transitions of CDs leading to improved luminescence with excellent thermal stability both in solution and solid states.

Introduction

Luminescent carbon dots (CDs) have attracted great attention due to their distinct benefits for bioimaging and lighting applications such as high photoluminescence (PL) quantum yield (QY), high photostability, excellent biocompatibility, low toxicity and low fabrication cost.[1–8] The PL of CDs can be related to conjugated sp^2-domains in their carbon cores,[9,10] molecular fluorophores,[11–13] or surface groups.[14–16] Surface modification of CDs is considered to be an effective way to tune their luminescence, so multiple efforts have been paid to exploit different protocols, mostly conducted through post-synthetic chemical treatment.[17–25] Chemical oxidation was widely used to adjust the band gap of CDs and to shift their emission to longer wavelengths. Bao *et al.* used an electrochemical method to increase the surface oxidation degree of CDs and realize red shifted emission without the change of CD core size.[19] Amine-based passivation could improve the emission of CDs.[20] The emission of CDs could even be shifted from red to the near-infrared *via* the surface interaction with sulfoxide/carbonyl-rich molecules.[17] Many of these procedures rely on the noncovalent bonding with surface modifier molecules, which is less stable and can be easily broken by external stimuli, such as heating or interaction with aprotic polar solvents, thus diminishing emission intensity of changing the PL peak position.

Herein, we have developed another kind of the surface modification strategy to tune the emission of CDs using cyanuric acid (CA), which is achieved *via* a simple co-crystallization process. Starting from the blue emissive CDs co-crystallized with CA in aqueous solution, the resulting composite material possesses strong green emission with PLQY of 62%, and shows room temperature phosphorescence in the solid state. Remarkably, when re-dissolved in water, the CA and CDs composite (CDs/CA) still exhibits green emission with PLQY of 24%, which remains unchanged under external thermal treatment in polar solvents at ambient conditions. At the same time, after further 7 h hydrothermal treatment at 160 °C, the blue emission from the CDs can recover. Our data indicate the co-crystallization process with CA molecules can effective modify the surface of CDs and directly influence the electron transitions of CDs, leading to the improved green emission.

Experimental section

Synthesis of CDs

Blue-emitting CDs were synthesized *via* a microwave assisted strategy as reported previously.[26] Citric acid (1 g) and thiourea

[a]*State Key Laboratory of Luminescence and Applications, Changchun Institute of Optics, Fine Mechanics and Physics, Chinese Academy of Sciences, Changchun 130033, PR China*
[b]*University of Chinese Academy of Sciences, Beijing 100049, PR China*
[c]*Department of Materials Science and Engineering, and Centre for Functional Photonics, City University of Hong Kong, Kowloon, Hong Kong SAR, PR China*
[d]*Center of Information Optical Technologies, ITMO University, Saint Petersburg 197101, Russia*
[e]*Beijing Advanced Innovation Center for Soft Matter Science and Engineering, Beijing University of Chemical Technology, Beijing 100029, PR China*
[f]*Joint Key Laboratory of the Ministry of Education, Institute of Applied Physics and Materials Engineering, University of Macau, Taipa, Macau, PR China.*
E-mail: songnanqu@um.edu.mo

†Electronic supplementary information (ESI) available. See DOI: 10.1039/d0nr02639e

(1 g) were dissolved in deionized water (DI, 20 ml), and the solution was heated in a domestic 650 W microwave oven for 5 min, resulting in a dark viscous solid. The product was dissolved in water, and centrifuged at 8000 rpm for 10 min to remove excessive large particles. The obtained dark brown supernatant was further centrifuged at higher speed (16 000 rpm) for 10 min to remove agglomerated nanoparticles, and then dialyzed against deionized water through a dialysis membrane (1000 Da) for 12 h. The CDs in a powdered form were separated from the solvent *via* freeze drying.

Preparation of CDs@CA crystals

CDs@CA crystals were prepared by dissolving CDs (2 mg) in a saturated aqueous solution (50 ml) of CA (2 g). The mixture was left at room temperature and crystals were gradually formed in this solution during 4 h. The obtained CDs@CA crystals were washed with deionized water, subjected to freeze drying, and grounded into a powder.

Cyclic voltammetry

Cyclic voltammetry (CV) measurements were performed using a BAS 100 W Bioanalytical System: a glass-carbon disk electrode was used as the working electrode, a Pt wire as the counter electrode, Ag/Ag^+ as the reference electrode and Bu_4NPF_6 (0.1 M) in *N*,*N*-dimethylformamide (DMF) as the electrolyte.

Materials and basic characterization techniques

Citric acid, thiourea and cyanuric acid were purchased from Beijing Chemical Reagent Company (China), are all used in the as-received condition without further purification. In all cases, the water (18.2 MΩ cm@25 °C) used in the experiments is purified with a Millipore system.

TEM was performed on a FEI Tecnai-G2-F20 TEM operated at 200 kV. XRD patterns are obtained with a Bruker AXS D8 Focus using Cu Kα radiation (λ = 1.54056 Å). X-ray photoelectron spectrometer using Mg as the excitation source. Fluorescence emission spectra were collected on a NOVA fiber-coupled spectrometer. Excitation–emission maps were collected on a Hitachi F-7000 spectrophotometer.

Absolute photoluminescence quantum yields (PL QY) were measured with a calibrated integrating sphere in an Otsuka QE-2000 spectrometer.

Optical absorption spectra and FT-IR spectra were recorded on a Shimadzu UV-3101PC spectrophotometer and a PerkinElmer spectrometer (Spectrum One B), respectively. Time-resolved PL spectra and phosphorescence spectra were measured by a LifeSpec-II dedicated lifetime spectrometer (Edinburgh Instruments).

Results and discussion

The morphology of CDs was characterized by transmission electron microscopy (TEM) and high-resolution TEM (HRTEM). As shown in Fig. 1a, the particles are close to spherical in shape and rather monodisperse, with an average size of 3 nm. HRTEM image (inset in Fig. 1a) shows that CDs exhibit lattice fringes with a spacing of 0.21 nm, which fits the (100) lattice space of graphitic carbon.[27] X-ray diffraction (XRD) pattern of the CD powder (Fig. S1a†) exhibits an intense peak located at 26.4°, corresponding to a layer spacing of 3.4 Å in the graphite-like layer structure, further proving the existence of CDs' graphite-like cores.[28]

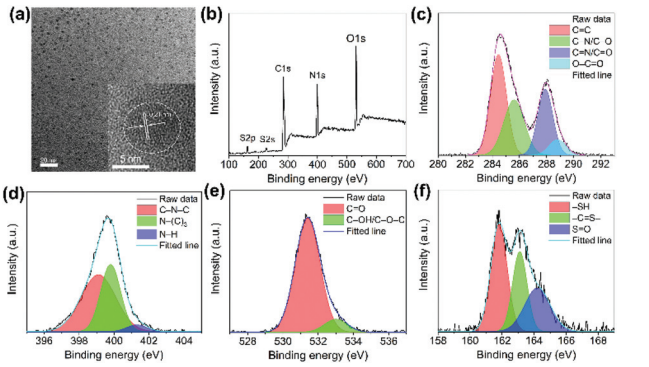

Fig. 1 (a) TEM image of CDs, with inset showing a representative HRTEM image of a single CD. (b) Full survey XPS spectra of CDs, with zoom-in XPS spectra for (c) C_{1s}, (d) N_{1s}, (e) O_{1s}, and (f) S_{2p} elements.

The chemical structure of CDs was investigated by Fourier transform infrared (FT-IR) spectroscopy and X-ray photoelectron spectroscopy (XPS). In the FT-IR spectra (Fig. S1b†), the broad absorption peak from 3600–3100 cm^{-1} is attributed to stretching vibrations of O–H and N–H groups. The strong absorption peak at 1704 cm^{-1} is assigned to the stretching vibration of C=O. The absorption peaks at 1574 cm^{-1} and 1403 cm^{-1} are attributed to the stretching of C=C bonds and C–N bonds, respectively. The weak peaks at 685, 1047 and 2487 cm^{-1} are attributed to the C–S, C=S and S–H vibration bonds, respectively.[29] The full survey XPS spectrum of the CDs (Fig. 1b) exhibits five peaks at 162.5, 226.7, 284.7, 399.6 and 531 eV, which are attributed to S_{2p}, S_{2s}, C_{1s}, N_{1s} and O_{1s}, respectively.[30] It shows that nitrogen and sulfur are co-dopants of the CDs, originating from thiourea used as a precursor. In the high-resolution XPS spectra acquired for each single constituting element (Fig. 1b–e), the C_{1s} spectrum has four peaks at 284.5, 285.6, 287.8 and 288.8 eV, which can be assigned to C=C, C–N/C–O, C=N/C=O and O–C=O bonds, respectively. The O_{1s} band contains two peaks at 531.6 and at 533 eV, belonging to the C=O and C–OH/C–O–C bonds, respectively. The N_{1s} spectrum shows existence of the C–N–C bond at 399.1 eV, N–$(C)_3$ bond at 399.8 eV and N–H bond at 401.3 eV. The spectrum of S_{2p} consists of three peaks at 161.8, 163.1 and 164.2 eV which can be assigned to –SH, –C=S– and S=O bonds, respectively. These data demonstrate that CDs surface contains amino, carboxyl, carbonyl and sulfur-containing groups, which should be able to bond with appropriate surface modifiers.

There have been previous reports that CA molecules could be used as a CDs matrix, leading to the enhanced fluo-

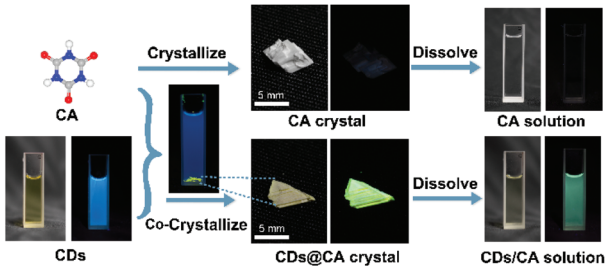

Fig. 2 Series of photographs illustrating co-crystallization of CA and CDs leading to the formation of the CDs@CA crystals, which can be further dissolved in water providing the CDs/CA aqueous solution. All photographs are taken under sunlight and UV light for the left- and right-handed positions, respectively.

rescence and phosphorescence of the resulting composite materials.[31,32] Considering that CDs contain abundant –OH, –SH, –NH groups on the surface, which could provide bonding sites for CA molecules, CDs embedded into CA crystals (we will denote these samples CDs@CA crystals further on) were prepared through a simple co-crystallization process by dissolving CDs in a saturated CA aqueous solution. The XRD pattern (Fig. S2a†) and SEM images (Fig. S3†) of the bare CA crystals and CDs@CA crystals were almost identical, indicating that the structure of the CA crystals was well preserved upon embedding CDs. As shown in Fig. 2, CA crystals and CDs@CA crystals exhibit white and yellowish colors under sunlight, respectively. CA crystals show no emission either in solution or in solid state, while strong green PL was observed from the CDs@CA crystals under UV light (Fig. 2). The maximum of the emission peak of CDs@CA crystals was at 525 nm (Fig. 3d), and the PL QY reached 62% under 420 nm excitation.

Remarkably, upon dissolving CDs@CA crystals in water (we will denote these samples CDs/CA solution further on) the resulting samples also possessed green emission, which was different from what was observed for the initial CDs, which had a blue PL (Fig. 2). Absorption spectra of aqueous solutions of CA, CDs and CDs/CA are shown in Fig. 3a. CA exhibited the main absorption band at 240 nm, and nearly no absorption after 320 nm. CDs had two absorption bands centered at 266 nm and 340 nm with a shoulder around 430 nm which are owing to the π–π* transition of the aromatic sp^2 domains and the n–π* transition of the C=O bonds, and optical transitions are assigned to surface groups, respectively. CDs/CA solution exhibited the same absorption bands as CDs solution in 340 nm and 430 nm, however, optical density of the band centered at 425 nm was greatly enhanced, which could be attributed to the changes on the surface of CDs after co-crystallization. The excitation–emission maps of CDs and CDs/CA in aqueous solutions are shown in Fig. 3b and c, respectively. The CDs showed an excitation-dependent emission with the strongest emission peaked at 445 nm (PL QY of 10%) under 360 nm excitation, which is consistent with literature.[26] In contrast, CDs/CA exhibited the strongest emission peaked at 525 nm with PL QY of 24% under 420 nm excitation. It can be seen

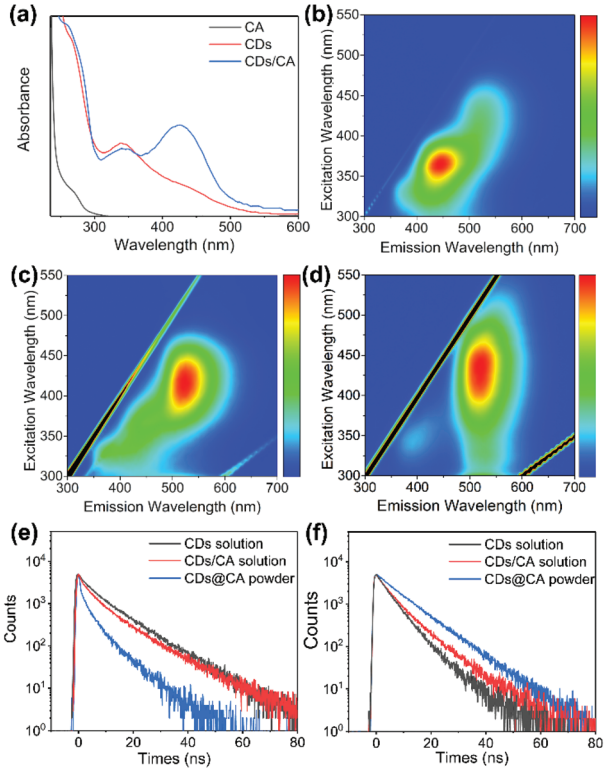

Fig. 3 (a) UV-Vis absorption spectra of CA, CD and CDs/CA aqueous solutions. Excitation–emission maps of (b) CDs aqueous solution, (c) CDs/CA aqueous solution, and (d) CDs@CA crystals. PL decay curves of aqueous solutions of CDs and CDs/CA, and of the CDs@CA powdered sample, which were (e) measured at 375 nm excitation and collected at 450 nm, and (f) measured at 405 nm excitation and collected at 525 nm.

that the emission of the CDs/CA aqueous solution experienced a strong bathochromic shift of 80 nm and the PL QY was enhanced 2.4 fold as compared with the original CDs. It can be suggested that even after re-dissolving CDs@CA crystals in water, the surface of CDs is still bonded with CA molecules, which could be a key reason for the modified optical properties of CDs.

PL decay curves measured for the CDs aqueous solution, CDs/CA aqueous solution and CDs@CA crystals are provided in Fig. 3. As shown in Fig. 3e, the average PL lifetime of the blue emission monitored at 450 nm (10.4 ns) decreased after bonding with CA molecules both in the aqueous solution (10.2 ns) and in powder (6.1 ns). In contrast, the average PL lifetime of the emerged green emission from CDs@CA crystals (9.0 ns) and CDs/CA aqueous solution (7.5 ns) monitored at 525 nm were increased compared to that from CDs aqueous solution (5.9 ns), indicating that the electronic structure of CDs has changed after bonding with CA, and the electronic transitions occur between CDs and CA.

The CDs@CA crystals obtained by the co-crystallization process also exhibited room temperature phosphorescence. As shown in Fig. 4a, green phosphorescence could be clearly observed from CDs@CA crystals by the naked eye after turning

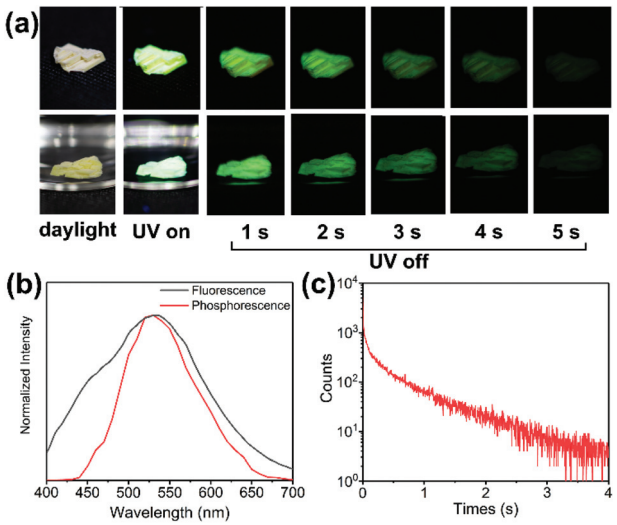

Fig. 4 (a) Bright field, fluorescence and phosphorescence photographs (from left to right) of CDs@CA crystals in the air (top) and in water (bottom). (b) Fluorescence and phosphorescence (collected after 50 ms) spectra of CDs@CA crystals excited at 360 nm. (c) Phosphorescence decay curve of CDs@CA crystals at room temperature measured at 360 nm excitation and collected at 525 nm.

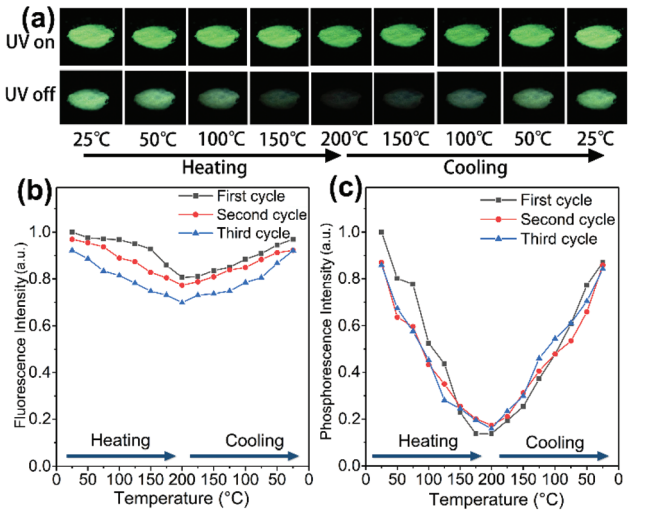

Fig. 5 (a) Photographs of CDs@CA powder under UV light (top) and after 100 ms of UV light turned off (bottom) at different temperature in heating and cooling process. Temperature dependencies of the emission intensity of the CDs@CA powder during three consecutive heating–cooling cycles: (b) fluorescence and (c) phosphorescence collected after 100 ms.

off the UV light for up to 5 s either in air or in water. As shown in Fig. 4b, the phosphorescence spectrum of CDs@CA crystals showed a similar emission peak centered at 525 nm as their fluorescence spectrum, but the half bandwidth of their phosphorescence spectrum is narrower than theirs fluorescence spectrum. The time-resolved phosphorescence signal from the CDs@CA composites excited at 360 nm and collected at 525 nm (Fig. 4c) showed that the average phosphorescence lifetime was 496 ms.

The fluorescence and phosphorescence intensities of the CDs@CA powder were examined during several heating–cooling cycles, as shown in Fig. 5. The temperature was increased step-wise from 25 °C to 200 °C, with every 25 °C interval lasting for 10 min, during which the fluorescence and phosphorescence intensities were measured. As shown in Fig. 5b and c, upon heating up to 200 °C, the fluorescence intensity of the CDs@CA powder was about 80% of its initial value at 25 °C, which can be recovered back with more than 95% from the initial signal after cooling to room temperature. In contrast, at 200 °C the phosphorescence intensity dropped down to 15% of the initial value at 25 °C, but was also recovered to about 88% after cooling to room temperature. The corresponding fluorescence and phosphorescence images under UV light excitation at different temperatures are shown in Fig. 5a, to illustrate and visualize the data shown in Fig. 5b and c. After three heating–cooling cycles, the fluorescence and phosphorescence intensities of the CDs@CA powder still remained 92% and 85% from the initial values, respectively, indicating the excellent thermal stability. It should be noted that the phosphorescence of the CDs@CA powder still remained at about 50% of the initial intensity and could be detected by naked eye even at 100 °C.

To investigate how stable the CA and CDs are bound together after the co-crystallization process, the UV-Vis absorption and PL spectra of pure CDs solutions, mixed CA and CDs solutions (we will denote these samples CDs + CA solutions further on) and CDs/CA solutions were measured at different temperatures. CDs + CA solutions were prepared by dissolving CDs in CA aqueous or DMSO solutions. The absorption and PL spectra of CDs and CDs + CA solutions exhibited similar spectra at the tested temperatures, which decreased slightly upon heating from 50 °C to 100 °C, and can be nearly completely recovered upon cooling back to 50 °C (Fig. S4†). No changes in the normalized absorption and PL spectra (Fig. 6a and b) were observed during the heating and cooling processes for these samples. The same optical behaviors of CDs solutions and CDs + CA solutions upon heating/cooling cycles indicate that the CA molecules cannot bond to the surface of CDs in solution, and thus do not affect luminescence properties of CDs. On the other hand, normalized absorption and PL spectra of the CDs/CA solutions in water (Fig. 6c and d) and DMSO (Fig. S5†) were nearly unchanged during the heating/cooling cycles, indicating that CA molecules can firmly bond to the surface of CDs through the co-crystallization process, which cannot be disrupted by dissolving them in polar solvents even upon heating to 100 °C at room pressure. To further test surface CA-bonded CDs, the CDs/CA aqueous solution was subjected to a more harsh treatment under hydrothermal conditions at 160 °C for different time. As shown in Fig. 6e and f, after hydrothermal heating at 160 °C for 1 h, 3 h, 5 h, 7 h and 9 h, the PL of the samples gradually changed from green to blue emission with the gradually decreased absorption band at 425 nm. The corresponding photographs under sunlight and UV light excitation are shown in Fig. S6,†

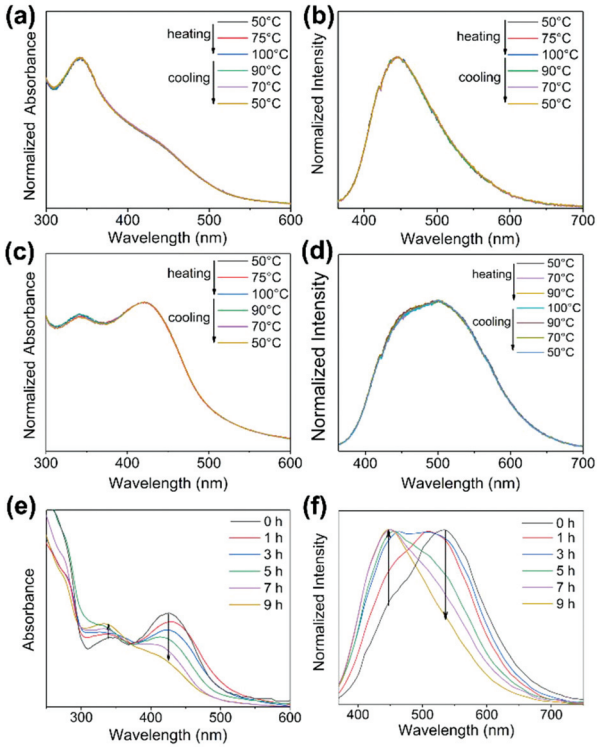

Fig. 6 Normalized UV-Vis absorption spectra of (a) CDs + CA and (c) CDs/CA aqueous solutions, and normalized PL spectra of (b) CDs + CA aqueous solution, (d) CDs/CA aqueous solution under 360 nm excitation measured at different temperatures in the heating and cooling process. (e) UV-Vis absorption and (f) PL spectra of CDs/CA aqueous solutions after hydrothermal heating at 160 °C for 0 h, 1 h, 3 h, 5 h, 7 h and 9 h.

to illustrate and visualize the data shown in Fig. 6e and f. It can be inferred that the surface bonded CA molecules were gradually removed from the CD surface under the hydrothermal treating, leading to the recurrence of the blue emission of the initial CDs.

To study the bonds between CA molecules and CDs, FT-IR spectra were analyzed. As seen in Fig. 7, the infrared absorption peaks of CA molecules in the bare CA crystals and CDs@CA

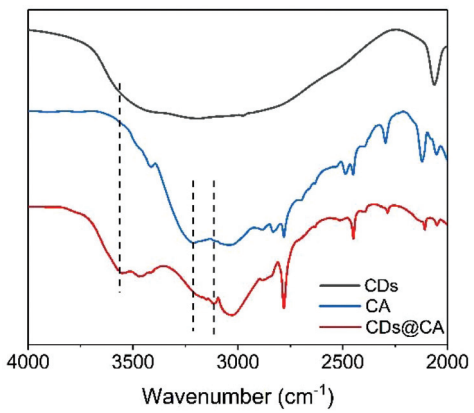

Fig. 7 FT-IR spectra of CDs, CA and CDs@CA powders.

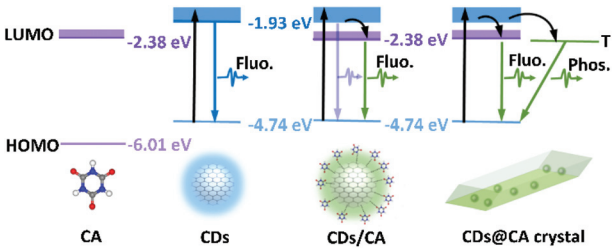

Fig. 8 Illustration of the co-crystallization induced surface modification, possible emission mechanisms, and energy levels alignment of CDs, CDs/CA and CDs@CA crystals.

crystals were roughly the same. The additional peaks in the region 3560–3500 cm^{-1} in the spectrum of CDs@CA can be assigned to the –OH vibrations from the embedded CDs. The –OH peak at 3220 cm^{-1} of the CA crystals moved to 3115 cm^{-1} in the CDs@CA crystals, indicating strengthened hydrogen bonds, which may happen during the co-crystallization process.

Cyclic voltammetry (CV) was employed to measure the HOMO and LUMO levels of CA, CDs and CD/CA in DMF. The oxidation onset potential and initial reduction potentials for CA and CDs were 1.77 eV and −1.86 eV, and 0.51 eV and −2.30 eV, respectively (Fig. S7†). Thus, CDs exhibited lower initial reduction potentials than CA. For CDs/CA composite, the oxidation onset potential and initial reduction potentials were at 0.50 eV and −1.85 eV, respectively. It should be noted that CDs/CA samples showed similar initial reduction potentials with CA. Thus, it can be inferred that CDs/CA and CA had similar LUMO levels, located at −2.38 eV (Fig. 8).

Based on the data obtained above, the co-crystallization induced surface modification of CDs with CA molecules is presented in Fig. 8. During the co-crystallization, CDs were embedded into CA crystal lattice and bonded with CA molecules through the hydrogen bonds which could not be broken after further dissolving in polar solvents and the heating at normal conditions. Based on the absorption and PL spectra measurements, and the CV measurements of CA, CDs, CDs/CA, we inferred that the surface bonded CA molecules affected the electron transitions of CDs, shifting LUMO level in CDs/CA to the value similar to that of CA. Thus, all photoexcited charge carriers relaxed from high energy levels to the LUMO level of surface bonded CA molecules, and then recombined to the HOMO level of CDs *via* emitting light in the green spectral region. In the CDs@CA crystals, due to the suppression of the vibrational and rotational motions of the organic groups at the CDs surface, the excited carriers may also undergo an intersystem crossing from the lowest singlet to the lowest triplet state, and then radiatively relax to the ground state, giving rise to the green phosphorescence.

Conclusions

In summary, a simple co-crystallization strategy was developed to modify the luminescence properties of CDs. By applying

this method, CDs@CA crystals with strong green photoluminescence (PLQY of 62%) and room temperature phosphorescence were obtained. During the co-crystallization process, the CA molecules firmly bonded to the surface of the CDs, which cannot be disrupted by polar solvents or temperature stimuli. The surface bonded CA molecules directly affected the optical transitions of CDs and resulted in the change of the blue emission to enhanced green emission. This study contributed new insights into the origin and modulation possibilities of the luminescence of CDs, and may promote their extended applications in various fields.

Conflicts of interest

There are no conflicts to declare.

Acknowledgements

This work was supported by the National Natural Science Foundation of China (No. 61975200), the Youth Innovation Promotion Association of CAS (No. 2018252), Jilin Province Science and Technology Research Projects (No. 20170101191JC and 20180101190JC), the Science and Technology Development Fund, Macau SAR (0040/2019/A1), NSFC's Excellent Young Scientists Fund (HK& Macau) (No. 61922091), funded by University of Macau (SRG2019-00163-IAPME), the Ministry of Science and Higher Education of the Russian Federation (Grant 14.Y26.31.0028), and by the RFBR Project No. 18-29-19122 mk.

References

1 Y.-P. Sun, B. Zhou, Y. Lin, W. Wang, K. A. S. Fernando, P. Pathak, M. J. Meziani, B. A. Harruff, X. Wang, H. Wang, P. G. Luo, H. Yang, M. E. Kose, B. Chen, L. M. Veca and S.-Y. Xie, *J. Am. Chem. Soc.*, 2006, **128**, 7756.
2 S. N. Baker and G. A. Baker, *Angew. Chem., Int. Ed.*, 2010, **49**, 6726.
3 H. Ding, S. Yu, J. Wei and H. Xiong, *ACS Nano*, 2016, **10**, 484.
4 S. Zhu, Q. Meng, L. Wang, J. Zhang, Y. Song, H. Jin, K. Zhang, H. Sun, H. Wang and B. Yang, *Angew. Chem., Int. Ed.*, 2013, **52**, 3953.
5 K. Hola, Y. Zhang, Y. Wang, E. P. Giannelis, R. Zboril and A. L. Rogach, *Nano Today*, 2014, **9**, 590.
6 M. Zheng, S. Liu, J. Li, D. Qu, H. Zhao, X. Guan, X. Hu, Z. Xie, X. Jing and Z. Sun, *Adv. Mater.*, 2014, **26**, 3554.
7 D. Li, D. Han, S. Qu, L. Liu, P. Jing, D. Zhou, W. Ji, X. Wang, T. Zhang and D. Shen, *Light: Sci. Appl.*, 2016, **5**, e16120.
8 X. Bao, Y. Ye, B. Zhang, D. Li, D. Zhou, P. Jing, G. Xu, Y. Wang, K. Holá, D. Shen, C. Wu, R. Zbořil and S. Qu, *Light: Sci. Appl.*, 2018, **7**, 91.
9 S. Qu, D. Shen, X. Liu, P. Jing, L. Zhang, W. Ji, H. Zhao, X. Fan and H. Zhang, *Part. Part. Syst. Charact.*, 2014, **31**, 1175.
10 C. Chien, S. Li, W. Lai, Y. Yeh, H. Chen, I. Chen, L. Chen, K. Chen, T. Nemoto, S. Isoda, M. Chen, T. Fujita, G. Eda, H. Yamaguchi, M. Chhowalla and C. Chen, *Angew. Chem.*, 2012, **124**, 6766.
11 Y. Xiong, J. Schneider, C. J. Reckmeier, H. Huang, P. Kasák and A. L. Rogach, *Nanoscale*, 2017, **9**, 11730.
12 F. Ehrat, S. Bhattacharyya, J. Schneider, A. Löf, R. Wyrwich, A. L. Rogach, J. K. Stolarczyk, A. S. Urban and J. Feldmann, *Nano Lett.*, 2017, **17**, 7710.
13 E. A. Stepanidenko, I. A. Arefina, P. D. Khavlyuk, A. Dubavik, K. V. Bogdanov, D. P. Bondarenko, S. A. Cherevkov, E. V. Kundelev, A. V. Fedorov, A. V. Baranov, V. G. Maslov, E. V. Ushakova and A. L. Rogach, *Nanoscale*, 2020, **12**, 602.
14 H. Ding, S. Yu, J. Wei and H. Xiong, *ACS Nano*, 2016, **10**, 484.
15 L. Bao, C. Liu, Z. Zhang and D. Pang, *Adv. Mater.*, 2015, **27**, 1663.
16 T. Yeh, W. Huang, C. Chung, I. Chiang, L. Chen, H. Chang, W. Su, C. Cheng, S. Chen and H. Teng, *J. Phys. Chem. Lett.*, 2016, **7**, 2087.
17 D. Li, P. Jing, L. Sun, Y. An, X. Shan, X. Lu, D. Zhou, D. Han, D. Shen, Y. Zhai, S. Qu, R. Zbořil and A. L. Rogach, *Adv. Mater.*, 2018, **30**, 1705913.
18 Z. Zhou, P. Tian, X. Liu, S. Mei, D. Zhou, D. Li, P. Jing, W. Zhang, R. Guo, S. Qu and A. L. Rogach, *Adv. Sci.*, 2018, **5**, 1800369.
19 L. Bao, Z. Zhang, Z. Tian, L. Zhang, C. Liu, Y. Lin, B. Qi and D. Pang, *Adv. Mater.*, 2011, **23**, 5801.
20 F. Yuan, Y. Wang, G. Sharma, Y. Dong, X. Zheng, P. Li, A. Johnston, G. Bappi, J. Z. Fan, H. Kung, B. Chen, M. I. Saidaminov, K. Singh, O. Voznyy, O. M. Bakr, Z. Lu and E. H. Sargent, *Nat. Photonics*, 2020, **14**, 171.
21 S. Zhu, J. Zhang, S. Tang, C. Qiao, L. Wang, H. Wang, X. Liu, B. Li, Y. Li, W. Yu, X. Wang, H. Sun and B. Yang, *Adv. Funct. Mater.*, 2012, **22**, 4732.
22 J. Shen, Y. Zhu, X. Yang, J. Zong, J. Zhang and C. Li, *New J. Chem.*, 2012, **36**, 97.
23 B. Qi, H. Hu, L. Bao, Z. Zhang, B. Tang, Y. Peng, B. Wang and D. Pang, *Nanoscale*, 2015, **7**, 5969.
24 H. Tetsuka, A. Nagoya, T. Fukusumi and T. Matsui, *Adv. Mater.*, 2016, **28**, 4632.
25 Q. Xu, T. Ma, M. Danesh, B. N. Shivananju, S. Gan, J. Song, C. Qiu, H. Cheng, W. Ren and Q. Bao, *Light: Sci. Appl.*, 2017, **6**, e16204.
26 H. Li, F. Shao, H. Huang, J. Feng and A. Wang, *Sens. Actuators, B*, 2016, **226**, 506.
27 T.-F. Yeh, C.-Y. Teng, S.-J. Chen and H. Teng, *Adv. Mater.*, 2014, **26**, 3297.
28 H. Guo, X. Wang, Q. Qian, F. Wang and X. Xia, *ACS Nano*, 2009, **3**, 2653.

29 X. Zhang, S. Sun, X. Sun, Y. Zhao, L. Chen, Y. Yang, W. Lü and D. Li, *Light: Sci. Appl.*, 2016, **5**, e16130.
30 D. Qu, M. Zheng, J. Li, Z. Xie and Z. Sun, *Light: Sci. Appl.*, 2015, **4**, e364.
31 Q. Li, M. Zhou, M. Yang, Q. Yang, Z. Zhang and J. Shi, *Nat. Commun.*, 2018, **9**, 734.
32 J. Tan, Y. Ye, X. Ren, W. Zhao and D. Yue, *J. Mater. Chem. C*, 2018, **6**, 7890.